Supporting Information

Abou Hamdan et al. 10.1073/pnas.1212258109

SI Text

Demonstration of Eq. 8. If we denote $I(t) = 1 - A(t)$ the concentration of inactive species, then the evolution equation is

$$dI(t)/dt = -k_a(t) \times I(t).$$

The inflection corresponds to $d^2I(t)/dt^2 = 0$, and we compute

$$\frac{d^2I(t)}{dt^2} = \left(k_a^2(t) - \frac{dk_a(t)}{dt}\right) \times I(t).$$

Because $I(t) > 0$, $d^2I(t)/dt^2$ equates to zero when the term within brackets cancels. QED.

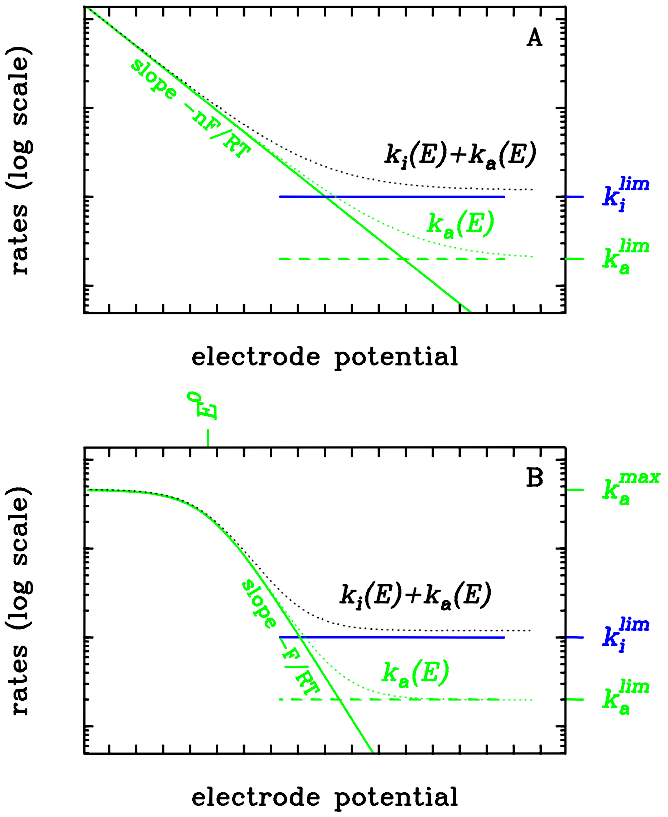

Fig. S1. (*A*) Variations of $k_a(E)$ and $k_i(E)$ defined in Eq. **3**. Note the *Y*-log scales. $k_a(E)$ (dashed green line) is the sum of a function that increases exponentially at low electrode potential and a constant k_a^{lim}. $k_i(E)$ (solid blue line) is constant and equates to k_i^{lim} over the entire range of *E*. In *B*, we illustrate the case where the one-electron exponential increase in k_a is the foot of a sigmoid that levels off at a value k_a^{max} when $E < E^0$.

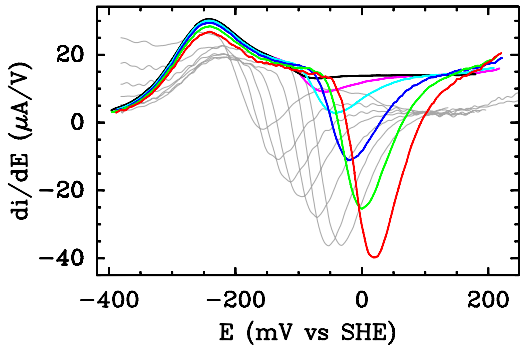

Fig. S2. Voltammetric characterization of the V74N mutant. Shown are derivatives of the data shown in Fig. 1*A* (solid colored lines) and Fig. S3 (gray lines).

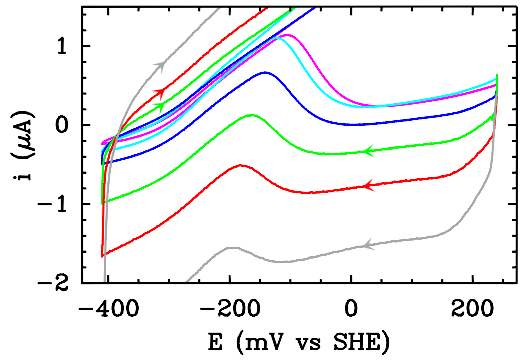

Fig. S3. Voltammetric characterization of the V74N mutant. These cyclic voltammograms (CVs) were recorded starting from the high-potential limit, after a 15-min (1,000 s) poise at high potential, at scan rates 5 mV/s (purple) and 10, 20, 40, 100, and 200 mV/s (gray). The first derivatives of the sweeps are shown in gray in Fig. S2, and the switch potentials are shown as open circles in Fig. 1*E*.

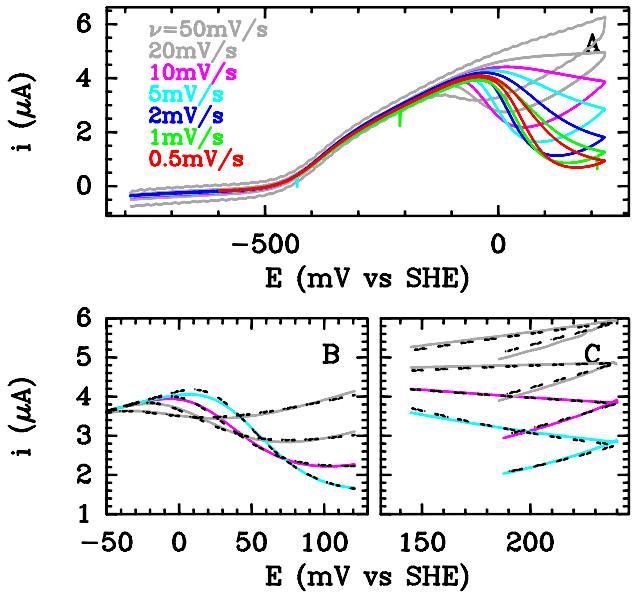

Fig. S4. Voltammetric characterization of the V74H mutant. (*A*) CVs recorded over a range of scan rates (from 50 to 0.5 mV/s, as indicated). (*B* and *C*) Fits to Eqs. **5** and **7** of fragments of the CVs shown in *A*. These gave the value of $1/\tau \approx k_i^{\lim}$ that is shown as a blue line in Fig. 2*C* and the rate of reactivation at low potential that is shown as a green line in Fig. 2*C*.

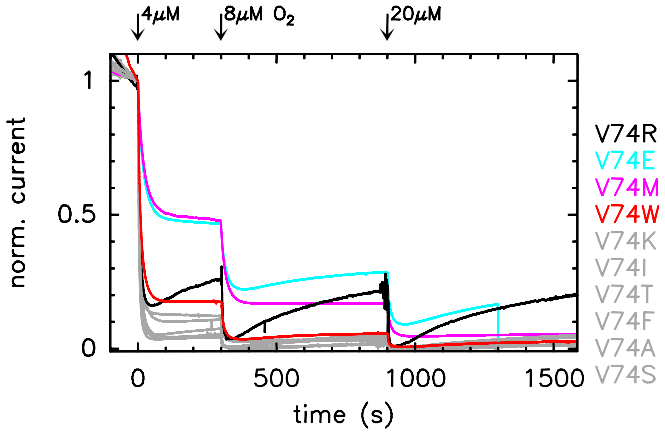

Fig. S5. Effect of transient exposure to O_2 on the turnover rate of mutants V74R, -E, -M, -F, -A, -K, -S, -T, and -I. All experiments were performed at 40 °C, $E = 140$ mV vs. SHE, pH 5.5, under 1 atm of H_2, $\omega = 3{,}000$ rpm.

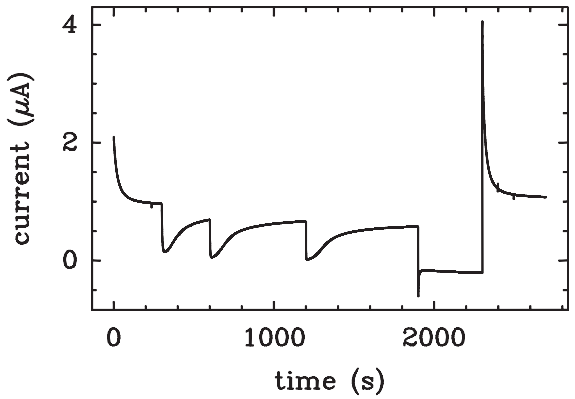

Fig. S6. Reaction with O_2 of the V74H mutants: The complete experiment shown in Fig. 4*A*. Exposure to O_2 was carried out at $+140$ mV. At $t = 1,900$ s, the potential was stepped to -560 mV. The value of the current recorded after the step back to $+140$ mV at 2,300 s shows that reactivation is complete. Here, the current includes the capacitive contribution.

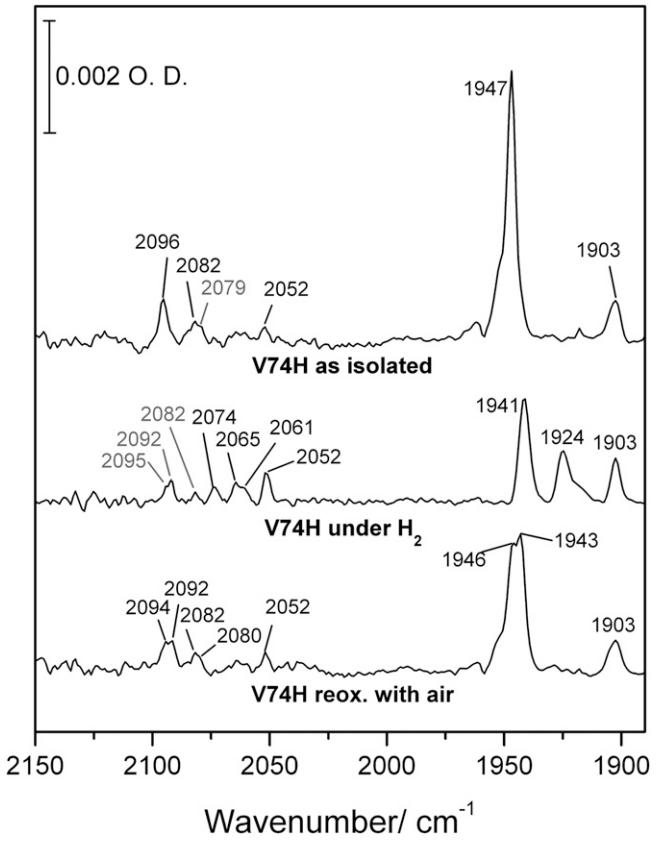

Fig. S7. FTIR characterization of the V74H mutant. The enzyme "as isolated" is mostly in the NiA state (1,947, 2,082 and 2,096 cm^{-1}), but it also shows an inert species with a CO band at 1,903 cm^{-1} and probably a CN band at 2,052 cm^{-1} (the other CN band being overlapped by others or not differentiated from the noise). Upon activation the RI and RII bands appear but with their CO frequencies shifted positively (2–3 cm^{-1}) relative to the wild-type ones (RI, 1,941, 2,061, and 2,074 cm^{-1} ; RII, 1,924, 2,052, and 2,065 cm^{-1}). In addition, in the reduced spectra there are several nonasigned CN bands in the 2,082- to 2,095-cm^{-1} range. They could correspond to the inactive enzyme (1,903 CO band) or to the shoulder observed at 1,920 cm^{-1}. Reoxidation with air leads to a mixture of NiB and a new state with a CO band at 1,943 cm^{-1}, one CN band probably at 2,094 cm^{-1}, and the other at 2,082 cm^{-1}, as in NiA.

Table S1. Kinetic properties of the V74 mutants of *D. fructosovorans* NiFe hydrogenase

Variant	Yield*	V_{max}, s^{-1} †	K_m, matm H_2 ‡	k_a^{-90mV}, s^{-1} §	Reference
WT	++	760 ± 100	10 ± 5	0.03	(1)
V74A	+	270 ± 20	30 ± 10	0.07	This work
V74C	+	1,050 ± 250	610 ± 300	1.5	(2)
V74D	+	280 ± 100	50 ± 20	0.25	(3)
V74E	+	340 ± 90	500 ± 200	0.25	(3)
V74F	+	800 ± 60	120 ± 60	0.03	(3)
V74H	++	750 ± 100	200 ± 50	30	This work
V74I	++	750 ± 100	130 ± 20	0.016	(4)
V74K	−		90 ± 20	0.2	This work
V74M	++	600 ± 60	300 ± 80	0.011	(5)
V74N	++	640 ± 55	300 ± 70	0.6	(2)
V74P	−		60 ± 15	0.85	This work
V74Q	++	860 ± 270	3,000 ± 1,000	0.44	(3)
V74R	−		60 ± 10	0.45	This work
V74S	++	400 ± 20	70 ± 15	0.16	(2)
V74T	++	620 ± 60	150 ± 40	0.025	This work
V74W	++	490 ± 100	280 ± 50	0.035	(3)

*The symbols "++ ", "+", and "−" indicate purification yields in the range 0.7–1, 0.3–0.6, and $\ll$0.3 mg of protein per liter of culture, respectively.

†The maximal rate of H_2 was measured at pH 8, 40 °C.

‡The Michaelis constants for H_2 oxidation were determined electrochemically (3). When the purification yield was too low, neither the concentration of protein nor the maximal rate of H_2 oxidation could be determined.

§The rate of anaerobic reactivation determined at −90 mV vs. SHE, pH 5.5, 40 °C.

1. Leroux F, et al. (2008) Experimental approaches to kinetics of gas diffusion in hydrogenase. *Proc Natl Acad Sci USA* 105(32):11188–11193.
2. Liebgott PP, et al. (2011) Original design of an oxygen-tolerant [NiFe] hydrogenase: Major effect of a valine-to-cysteine mutation near the active site. *J Am Chem Soc* 133(4):986–997.
3. Liebgott PP, et al. (2010) Relating diffusion along the substrate tunnel and oxygen sensitivity in hydrogenase. *Nat Chem Biol* 6(1):63–70.
4. Leroux F, et al. (2010) Is engineering O_2-tolerant hydrogenases just a matter of reproducing the active sites of the naturally occurring O_2-resistant enzymes? *Int J Hydrogen Energy* 35: 10770–10777.
5. Dementin S, et al. (2009) Introduction of methionines in the gas channel makes [NiFe] hydrogenase aero-tolerant. *J Am Chem Soc* 131(29):10156–10164.